Postprint of: Eremeev V., Balandin V., Balandin V., Bragov A., Konstantinov A., Igumnov L., Experimental study and numerical simulation of the dynamic penetration into dry clay, CONTINUUM MECHANICS AND THERMODYNAMICS (2023), pp. 1-13

V. A. Eremeyev · Vl. Vas. Balandin · Vl. Vl. Balandin · A.M.Bragov · A. Yu. Konstantinov · L. A. Igumnov

Experimental study and numerical simulation of the dynamic penetration into dry clay

Abstract Tests of dry clay were carried out in a uniaxial stress state using the experimental setup which implements the split Hopkinson pressure bar method. Based on the results of these experiments, the compressive strength of clay was determined as an important element of S.S. Grigoryan's model of the soil medium. In addition, the parameters of this model are determined from the results of experiments using the modified Kolsky method with a sample enclosed in a rigid cage. To verify the model of the soil medium, special experiments were carried out on the penetration of striker with conical tips into dry clay in a reversed settings. Using this identified model in the LS-Dyna software package, numerical simulation of penetration into clay was carried out under conditions similar to those carried out the reversed experiments. Comparison of the results of physical and numerical experiments showed their satisfactory agreement at a dry friction coefficient of 0.5.

Keywords Dry clay · Strain rate · Dynamic indentation · Measuring bar · Numerical simulation · Material model

V. A. Eremeyev · Vl. Vas. Balandin · Vl. Vl. Balandin · A. M. Bragov · A. Yu. Konstantinov (✉) · L. A. Igumnov
National Research Lobachevsky State University of Nizhny Novgorod, 23 Prospekt Gagarina (Gagarin Avenue) BLDG 6, Nizhny Novgorod 603950, Russian Federation
E-mail: konstantinov@mech.unn.ru

V. A. Eremeyev
E-mail: eremeyev.victor@gmail.com

Vl. Vas. Balandin
E-mail: vbalandin99@gmail.com

Vl. Vl. Balandin
E-mail: rustydog2007@yandex.ru

A. M. Bragov
E-mail: bragov@mech.unn.ru

L. A. Igumnov
E-mail: igumnov@mech.unn.ru

V. A. Eremeyev
Gdansk University of Technology, ul Narutowica, 11/12, 80-233, Gdansk, Poland

1 Introduction

The study of the impact interaction of deformable and solid bodies with soil media is of great scientific and applied importance. When studying the mechanisms of penetration into soils, computational methods are widely used. These methods make it possible to comprehensively model impact processes. When performing calculations, various software systems are used: LS-Dyna, Ansys, Logos, Abaqus, etc. Analytical methods are also often used to determine the main characteristics of penetration processes [1–4]. These methods make it possible to obtain penetration characteristics (resistance force, penetration depth, etc.) in the form of analytical functions. However, to obtain adequate results from numerical and analytical methods, it is necessary to carefully select existing mathematical models and set their parameters that most fully reflect the dynamic properties of interacting media. This requires a wide range of experimental studies of the dynamic properties of soil media.

It should be noted that for a number of soil media, the dynamic properties have been studied quite fully. In particular, for sand, using two complementary techniques—a plane-wave impact experiment and a modified Kolsky method with tests in a rigid cage—compressibility curves were obtained in a wide range of load amplitudes [5–15], and its shear properties were studied [16–18]. In these works, for a sandy medium, the influence of humidity and granulometric composition on the parameters of the shock adiabat, deformation diagrams, and shear resistance at high strain rates of 10^2–10^5 s^{-1} and load levels up to 5 GPa was studied. The data obtained make it possible to equip mathematical models of sand deformation and accurately set their parameters in a wide range of load changes depending on its initial physical and mechanical characteristics of sand. A detailed review of experimental studies of the dynamic properties of sand is given in [19].

There are relatively few data on the deformation of clay soils under dynamic impacts. In [20], in experiments using the Kolsky method, deformation diagrams were determined for clay samples under uniaxial stress. Clay samples were preliminarily statically loaded at various load levels. The experiments were carried out at strain rates from 60 to 600 s-1 and stress levels up to 4 MPa. An increase in the dynamic strength of the specimens and in the fracture strain with an increase in the strain rate and preload was found. The authors of [21] conducted a study of wet clay using the SHPB method in the stress range up to 12 MPa. Based on the data obtained, the parameters of the soil yield strength in the Mohr–Coulomb form are determined. In [22], in the pressure range up to 3.5 GPa, the impact compressibility of clay with different water content (0%, 4.8%, 7.5% and 10%) was studied. According to the results of the experiments, the parameters of the shock adiabats were determined, which turned out to be practically the same for different water contents in the samples. In [23], plane-wave experiments were carried out to determine the shock compressibility of loess, the density of which was 1.8 g/cm3 and the degree of saturation with water was 22%. The shock adiabat was obtained at stress levels from 0.2 to 1.6 GPa.

In [24], by the SHPB method dynamic studies of plasticine, simulating wet clay soil, are given. Diagrams of deformation of samples in a rigid cage in the range of longitudinal stresses up to 150 MPa are obtained. The parameters of the Mohr–Coulomb equation for the yield strength of plasticine are determined. In [25], the dynamic properties of wet clay samples in a rigid holder were studied. The experiments were carried out on an installation with SHPB in the range of longitudinal stresses up to 200 MPa. Compressibility curves and dependences of shear stresses on pressure in the Mohr–Coulomb form are obtained. Plane-wave experiments were also carried out to determine the shock adiabat of wet clay in the pressure range up to 2 GPa. In [26], a study was made of the dynamic compressibility and shear strength of dry clay, and the parameters of the S.S. Grigoryan's model for this environment. To verify the obtained parameters of the model, numerical simulation of the dynamic compression of the sample in the bounding cage was carried out. A good agreement between numerical and experimental results is obtained. However, for a more reliable verification of this model, it is necessary to conduct experiments of a different type, in particular, experiments on the penetration of solid and deformable bodies into clay. The analysis performed showed that there are a fairly large number of experimental results on the intrusion into sand of different moisture content [27–29]. However, for clayey soils, data on penetration are insufficient [30–38].

It should be noted that the existing data on the penetration of solids into clay soils are limited mainly by experiments with a model medium—plasticine. In [30], experiments were carried out on the penetration of conical tips with opening angles of 30° and 60° into a plasticine target in a direct setup in the speed range up to 200 m/s. An accelerometer placed on the penetrating body was used to determine the penetration resistance force.

In [31], the penetration resistance forces were determined for cones with opening angles 2α equal to 30°, 60°, 90° and 180° in the speed range up to 20 m/s. It was noted that the maximum drag force is achieved when the conical part of the striker is completely immersed and it is a power-law function of the impact velocity.

In [32], the penetration of conical impactors into plasticine was studied in the range of impact velocities of 30–300 m/s. A method was proposed for determining the maximum shear stresses τ_s that arise in the soil during the penetration of cones, according to the experimental dependences of the maximum penetration depth on the impact velocity, assuming that the penetration resistance force is determined only by the action of shear stresses on the surface of the penetrating body, and the velocity head (proportional to the square of the velocity) can be neglected. In [33], based on the results of measuring the final penetration depth of cones with half-opening angles of 15°, 30°, 45° and 90° into plasticine, the parameters of the two-term penetration equation in the Poncelet form were determined. The experiments were carried out at impact velocities from 50 to 400 m/s. In works [34–36], a study was made of the penetration of conical impactors into plasticine. Experiments with conical impactors (opening angle 2α =30°) were carried out at impact velocities from 20 to 86 m/s. The resistance forces were measured in different areas of penetration (non-stationary and quasi-stationary). Based on the data obtained, the dependences of the resistance coefficient and the soil shear strength parameter on the velocity in the two-term Poncelet equation were constructed.

In [37], in the reversed experiments, the penetration of a hemispherical head and cones with different vertex angles into plasticine was studied. The impact velocities varied in the range from 80 to 460 m/s. The maximum forces acting on the heads in the initial, non-stationary stage of penetration are determined. The maximum forces increase according to a power law with an increase in the impact velocity.

It should be noted that plasticine models the behavior of water-saturated clay soil. There are practically no experimental data on penetration for clay. It is worth noting the work [38], in which the forces acting on a cylindrical projectile with a conical tip (cone opening angle 60°) were experimentally determined when it penetrated clay in the range of impact velocities from 3 to 6,1 m/s. An analytical penetration model was proposed that takes into account the shear strength of the soil and friction on the surface of the projectile. Since the impact velocities were low, the soil was considered incompressible. The obtained analytical dependencies were numerically integrated. The authors noted good agreement between experimental and analytical results and suggested that this technique may be suitable for determining shear strength from a known impact velocity and maximum penetration depth. There are no data on the impact interaction of solids with dry clay targets.

2 Methods of experimental research

2.1 SHPB method

In [26], an experimental study of the deformation of dry clay under conditions of a three-dimensional stress state was carried out. For this, a modification of the Kolsky method was used, in which the sample is tested in an elastic confining cage. This type of testing made it possible to determine the volumetric compressibility curve of clay; however, clay, unlike sand, has structural strength and resists deformation even under uniaxial stress conditions. To refine the model and expand the class of problems for which it can be applied, in the present study, dry clay samples were tested under uniaxial compression conditions. For this, the well-known Kolsky method (split Hopkinson pressure bar) was used in its traditional implementation [39].

The mathematical SHPB model considers a system of three bars: two infinitely strong, endless and thin bars and one "soft" and very short (sample) between them. It is assumed that there is no wave dispersion and strain profile is uniformly distributed over cross section of the bar. Lateral oscillations of the bar particles are neglected. In one of the bars, a one-dimensional elastic wave $\varepsilon^I(t)$ is generated, which propagates in bars with velocity C. Wave propagation in the SHPB is presented by the x∼t diagram in Fig. 1. When the wave reaches the sample, it splits into two ones because materials of the bar and the sample possess different acoustic stiffness ρC. The first wave $\varepsilon^R(t)$ is reflected back, and the second wave $\varepsilon^T(t)$ passes through the sample and enters the second bar. The sample experiences elastoplastic deformation while the bars undergo elastic deformation. Amplitudes and shapes of the waves $\varepsilon^R(t)$ and $\varepsilon^T(t)$ are dependent on the ratio between acoustic stiffness of the bar and the sample and on response of the sample material to dynamic load applied. By recording these elastic waves with gauges and using formulas proposed by Kolsky, we can define how stress, strain and strain rate change in the sample with time.

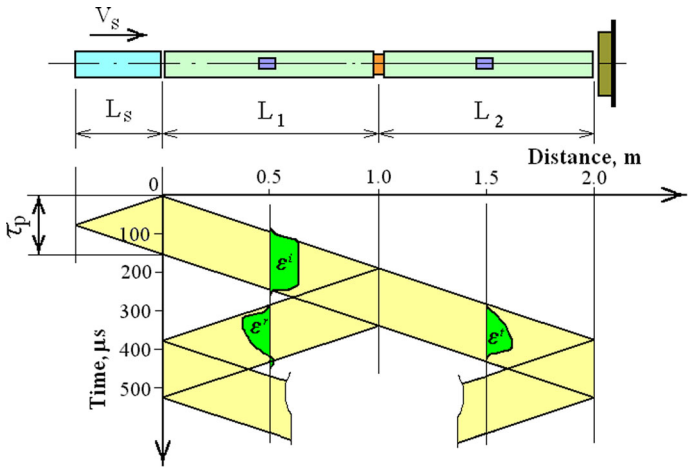

Fig. 1 Scheme of a setup that implements the split Hopkinson pressure bar method

Strain, strain rate and stress in the test sample were determined by formulas (1)–(3):

$$\varepsilon_s(t) = \frac{C}{L_0}\int_0^t \left[\varepsilon^I(\tau) - \varepsilon^R(\tau) - \varepsilon^T(\tau)\right] d\tau \tag{1}$$

$$\dot{\varepsilon}_s(t) = \frac{C}{L_0}\left[\varepsilon^I(t) - \varepsilon^R(t) - \varepsilon^T(t)\right] \tag{2}$$

$$\sigma_s(t) = \frac{E_b A_b}{A_s^0}\varepsilon^T(t) \tag{3}$$

where C is the speed of sound in the measuring bars, E_b is the Young modulus of the material of the bars, A_b is the cross-sectional area of the measuring bars, A_s^0 is the initial cross-sectional area of the sample, and $\varepsilon^I, \varepsilon^R and \varepsilon^T$ are the strains in the incident, reflected and transmitted strain pulses in the measuring bars. Excluding time as a parameter from the above dependences, one can obtain deformation diagrams $\sigma(\varepsilon)$ with a known history of changing loading conditions, namely the strain rate.

2.2 The technique of reversed experiment

The reversed experiments were carried out on the setup with 57-mm gas gun [27,28]. In the reversed experiment, the resistance force was measured at the initial penetration site. The method for measuring the force of resistance to the penetration of a striker into the sand using a measuring bar is as follows. The container filled with soil accelerates to the required speeds and strikes a fixed striker of the appropriate shape, fixed on a measuring bar. The impact velocity and the material properties of the bar must be such that plastic deformations do not occur in the bar. In this case, an elastic strain impulse $\varepsilon(t)$ is formed in the bar. The registration of this pulse makes it possible to determine the force F acting on the striker when interacting with the medium, according to the known relation $F(t) = \varepsilon(t)ES$, where E is the elastic modulus of the bar and S is the area of its cross section. Thus, in this method, the task of measuring forces is greatly simplified and is reduced to registering the elastic deformation impulse in the bar using strain gauges. The scheme of the installation which implements this method is shown in Fig. 2. In the proposed version of the reversed experiment, a 57-mm caliber gas gun with a double-diaphragm shutter is used to accelerate a container with soil, which makes it possible to obtain stable and easily controlled impact velocities in the range from 50 to 500 m/s. The container is a glass made of polypropylene filled with soil medium. The bottom of the container is glued to the cylindrical part. The impact speed of the container was measured using two electrical contacts located in the holes of the barrel, drilled in front of its muzzle. To close the contacts of the speed meter, an aluminum alloy ring was glued to the front edge of the container. The ratio of the distance between the contacts and the time of their closing gives the speed of the container before hitting the measuring bar.

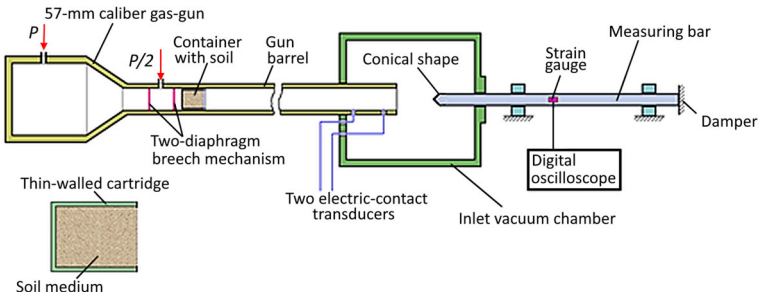

Fig. 2 Schematic representation of the setup for measuring forces resisting penetration in the reversed experiment

A steel bar 1.5 m long and 12 mm in diameter with a yield strength of more than 600 MPa is used for measuring forces by using a measuring bar technique. The impact end of the measuring bar had a conical shape with an angle at the top of 60°. The impact velocity was about 200 m/s. The rod is located at a certain distance from the muzzle of the barrel so that the impact occurs immediately after the full departure of the container from the barrel. The support, on which the rod is located, has adjusting supports, which allows to ensure the axisymmetric nature of the interaction. The rod with its rear end rests against a special stop, preventing its displacement and damping the impact energy. The impact occurs in a vacuum chamber to which the gun barrel is attached and into which a measuring rod is inserted. The geometric dimensions of containers with clay samples are shown in Fig. 3. The numbers indicate: 1—clay sample, 2—polypropylene container and 3—fragment of a measuring rod with a head.

2.3 Preparation of test specimens

Clay for testing was taken from a depth of 1 m in the Bogorodsky district of the Nizhny Novgorod region. The clay was dried in air at room temperature for a long time to completely remove moisture. Then pieces of dry clay were crushed to a powder. To form samples, ground clay was mixed with water in an amount of 20% by weight of the clay. The wet clay was thoroughly mixed to ensure uniformity. For testing by the SHPB method, clay samples were molded in special cylindrical holders in the same way as in [26]. A strictly defined mass of wet clay was placed in a holder between two punches. Then the punches were brought as close as possible to obtain the required volume of the sample. After forming the sample, the upper punch was removed from the holder. Then the samples were dried in air until the added moisture was completely removed. It should be noted that, upon evaporation of moisture, the samples decreased in length and diameter. With complete evaporation of water, the diameter of the samples was 16.5–16.7 mm, and the length was 12.5–12.6 mm. The density of the samples was 1940–2000 kg/m^3.

Clay samples for the reversed experiments were 70 mm high. The samples were molded in aluminum cylindrical containers with an inner diameter of 54 mm. During the formation of the samples, the wet clay was compacted to eliminate possible voids. Then these samples were removed from the container and dried in air until the added moisture was completely removed. When the moisture evaporated, the samples decreased in diameter, so the diameter of the container in which the samples were formed was chosen so that when the water completely evaporated, the diameter of the samples was close to 50 mm and corresponded to the inner diameter of the polypropylene test container. The density of the samples was 1940–1980 kg/m^3.

3 Results of the experimental study

3.1 The results of the SHPB tests

Figure 4 shows the results of studying the effect of strain rate on dry clay deformation diagrams under shock compression under uniaxial stress. The studies were carried out using the traditional Kolsky method. The loading conditions (deformation rate) were varied by changing the impactor speed. Data were obtained in the range of strain rates from 950 to 1300 1/s. Figure 4a shows a group of diagrams obtained under similar loading conditions, and Fig. 4b shows the dependence of the tensile strength of the material on the strain rate. It can be seen that the strain rate does not significantly affect the ultimate strength of the material under uniaxial

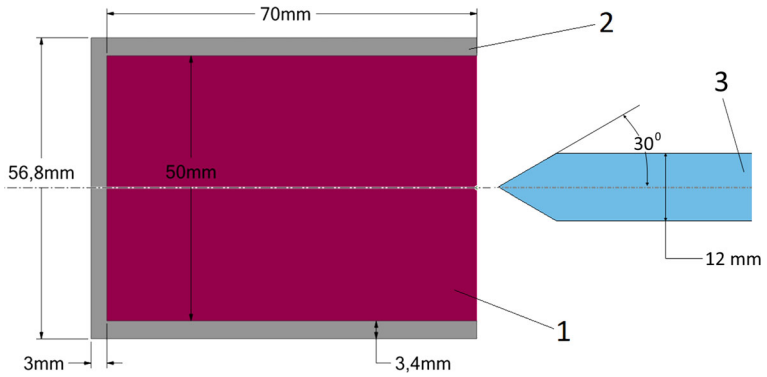

Fig. 3 Geometric dimensions of the sample and conical head

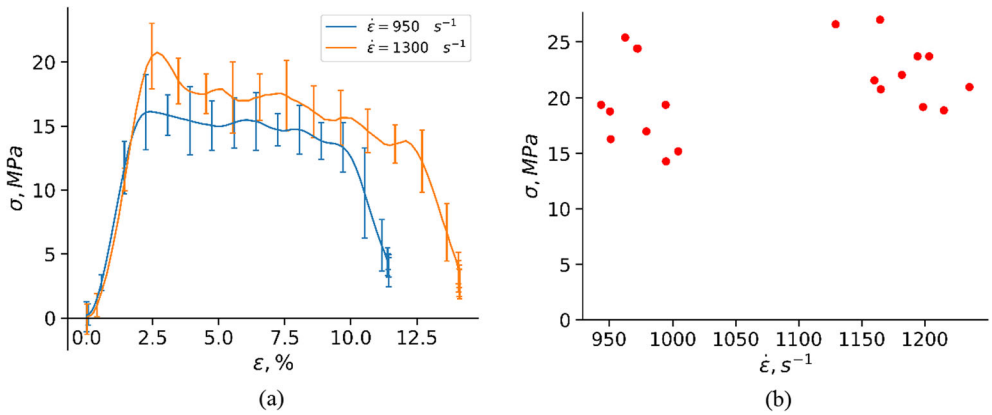

Fig. 4 **a** Deformation curves of dry clay under compression (strain rate −950 and 1300 1/s). **b** Rate dependence of the flow stress of dry clay under uniaxial compression

compression. Taking into account the scatter of experimental data, the ultimate strength values are in the range from 15 to 25 MPa.

3.2 The results of modified SHPB tests with cage

A description of the test procedure, sample preparation and experiments performed is given in [26]. The results of tests of clay samples in a bounding cage are shown in Fig. 5. The tests were carried out at a striker speed of 20 to 30 m/s. It can be noted that the nature of the volumetric compressibility curves (left side of the figure), as well as the dependence of stress intensity on pressure (Fig. 5a), is practically independent of the loading rate. In the deformation diagrams, the unloading curves differ significantly from the load ones. The load branches of the diagrams are actually repeated for different load amplitudes (impactor speed). Only the maximum deformation (and, accordingly, pressure) achieved in the test differs. At the highest strain rate, maximum pressures of the order of 250 MPa arise in the sample. The dependences of stress intensity on pressure (Fig. 5b) in the loading section are almost linear. The slope of these sections is practically independent of the loading rate.

3.3 Analysis of the results of the reversed experiment

To verify the model of the soil environment, several model experiments were carried out in an inverted formulation on the penetration of conical heads with a diameter of 12 mm in the inverted formulation described above into dry clay with a density of $1.94 \cdot 10^3$ kg/m^3 at impact velocities of about 200 m/s. The conditions for the experiments are given in Table 1. The dependences of the resistance forces on time were obtained (Fig. 6). In the figure, the colored lines show the results of repeated tests. The black line corresponds to the mean value. Confidence intervals with a probability of 0.95 are also shown. It can be noted that the increase in

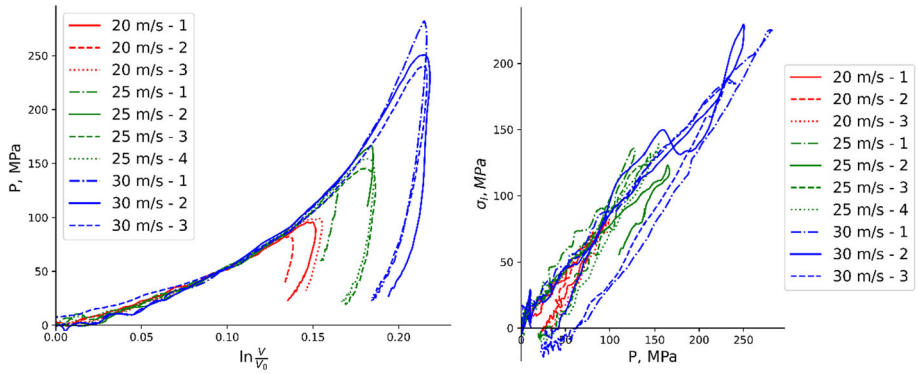

Fig. 5 **a** Volumetric compressibility curves, **b** the dependence of the yield strength on pressure

Table 1 Conditions of reversed experiments

No exp	Density. kg/m^3	Velocity, m/s	Fmax, kN
657	1940	188	20.6
659	1970	201	20.0
660	1980	208	20.2
661	1970	210	19.0

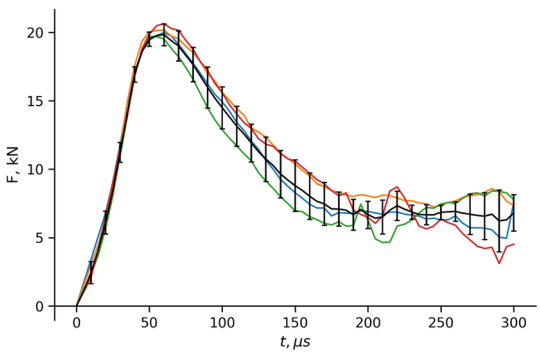

Fig. 6 Dependences of penetration resistance forces on time

the resistance force during the introduction of a cone with an angle of $2\alpha = 60°$ occurs along a curve close to a parabola. The maximum force during the introduction of the cone is reached at a moment close to the moment of immersion of the base of the cone. The maximum resistance forces in all the experiments performed are close. After reaching the maximum, there is a gradual decrease in strength, because the influence of the walls on the resistance force is small.

4 Numerical simulation

4.1 Mathematical deformation model of clay

A constitutive relation in the form of Grigoryan's model was chosen for modeling the clay behavior [40]. This model is widely used to simulate the behavior of soft soil media under dynamic loads. Soft soil is considered as an elastoplastic medium that provides nonlinear resistance to compression and shear [41]. In this model, to describe the nonlinear behavior of the soil medium, it is necessary to specify the dependence of pressure on volumetric deformation (or density), as well as the dependence of the flow stress on pressure.

In LS-DYNA computational code, a similar model is implemented in the form of material: MAT_SOIL_AND_FOAM [42]. This is a fairly simple model and is recommended for describing soils, concretes and foams.

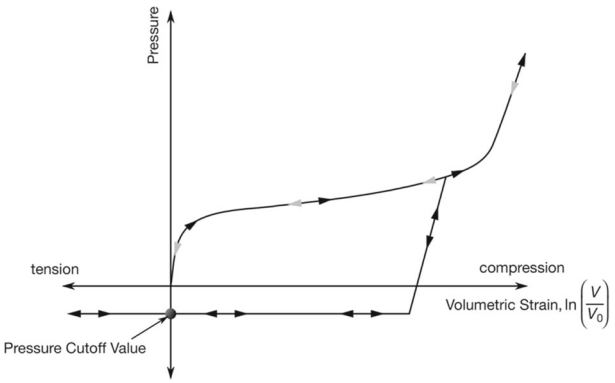

Fig. 7 Curve of volumetric compressibility in the MAT_SOIL_AND_FOAM model [34]

The volumetric compressibility curve is shown schematically in Fig. 7. As part of the model implementation in LS-DYNA, there are two options for material behavior during unloading. In the first case, unloading occurs along the same curve as the load (gray arrows in Fig. 7). In the second, unloading is performed in a straight line, the slope of which is set by the module of all-round compression K. During tension, the maximum pressure is limited by the *Pressure Cutoff*.

The pressure is considered positive when compressed. Volumetric deformation is determined by the natural logarithm of the relative volume (4).

$$e = ln\frac{V}{V_0} \tag{4}$$

where V is the current volume, V_0 is the initial volume.

The $P(e)$ curve is specified as a table function.

The plastic behavior of the medium is described using the ideal plastic flow function (5).

$$\phi = J_2 - \left[a_0 + a_1 P + a_2 P^2\right] \tag{5}$$

where J_2 is the second invariant of the stress tensor deviator (6).

$$J_2 = \frac{1}{2} s_{ij} s_{ij} \tag{6}$$

where s_{ij} are the components of the stress tensor deviator.

On the flow surface:

$$J_2 = \frac{1}{3}\sigma_Y^2 \tag{7}$$

where σ_Y is the flow stress at a uniaxial stress state.

Thus,

$$\sigma_Y = \left[3\left(a_0 + a_1 P + a_2 P^2\right)\right]^{1/2} \tag{8}$$

The considered model does not imply strain hardening. The plastic behavior of the material is determined by the values of the material parameters a_0, a_1, a_2.

Model identification for clay was carried out on the basis of data obtained during the experimental determination of the dynamic compressibility of clay using a modified SHPB method described above.

As a result of the performed experimental studies, the dependences of pressure on volumetric deformation, as well as stress intensity on pressure, were obtained for three loading modes, which correspond to striker velocities of 20, 25, and 30 m/s. The dependences of pressure on the logarithm of the relative volume of the sample, grouped by loading modes, are shown in Fig. 5a. There is a good repeatability of the results of experiments carried out under the same conditions. Figure 5b illustrates the shear stress as a function of pressure for three loading modes. It can be noted that the nature of volumetric compressibility curves is practically independent of the loading rate. It should be noted that the unloading curves in the deformation

Table 2 Dependence of pressure on volumetric deformation

$\ln \frac{V}{V_0}$	0	−0.05	−0.1	−0.125	−0.15	−0.175	−0.2	−0.22
***P*, MIIa**	0	20	53	75	105	150	220	275

Table 3 Complete set of model constants

ρ, kg/m^3	G, MPa	K, MPa	a_0, $MIIa^2$	a_1, MIIa	a_2
1980	5200	11383	75	8.26	0.227

diagrams differ significantly from the load ones. The load branches of the diagrams are actually repeated for different load intensities. The only difference is the maximum volumetric deformation achieved in the test (and, accordingly, the pressure). At the highest strain rate, maximum pressures of the order of 250 MPa appear in the sample. Dependences of stress intensity on pressure in the loading section are practically linear. The slope of these sections is practically independent of the loading rate.

The data shown in Fig. 6 were approximated to equip the MAT_SOIL_AND_FOAM model with the necessary parameters and constants. The table function is presented in Table 2.

Unloading within the framework of the considered model is carried out along a straight line with a given inclination angle. The modulus of the unloading branch was determined by approximating the experimental data. The modulus of volumetric compression K during unloading was 11383 MPa.

The procedure for determining the parameters of the Grigoryan's model based on the test data of soft soils in the limiting cage is described in [43].

The loading path parameters on the stress plane under conditions of a uniaxial deformed state can be obtained analytically. The loading path is formed by three segments. The first segment corresponds to the plastic loading of the soil from zero in the initial state to the maximum stress value, determined by the amplitude of the load pulse. The second segment corresponds to the elastic deformation of the soil at the initial stage of unloading from the achieved state. The third segment is associated with the transition of the soil from elastic to plastic state.

The slope of the first section is related to the lateral pressure coefficient (determined experimentally), which in turn is related to the coefficient in the linear dependence of the yield stress on pressure. The dependence of the flow stress on pressure (Fig. 5b) is well described by a linear function (9).

$$\sigma_Y = k \cdot P + b = 0.81 \cdot P \tag{9}$$

The coefficients of the MAT_SOIL_AND_FOAM model are determined by equations (10).

$$a_0 = \frac{\sigma_0^2}{3} \cdot a_1 = \frac{2.k\sigma_0}{3}, a_2 = \frac{k^2}{3} \tag{10}$$

where σ_0 is the dynamic yield stress of clay, determined by using the classical version of the SHPB method in compression under conditions of a uniaxial stress state.

The complete set of model constants for σ_0 =15 MPa is presented in Table 3.

4.2 Numerical simulation of the reversed experiment

The geometric composition of the problem corresponds to the experimental scheme shown in Fig. 3. A sample with a length of 70 mm and a diameter of 50 mm was tested on an setup with a measuring bar with a diameter of 12 mm. The samples were placed in a polypropylene cage. In the figure, the numbers are indicated: 1—sample, 2—container and 3—fragment of a measuring bar with a conical head. The cone angle is 60 degrees. Sample 1 in container 2 is accelerated using a gas gun. In the simulated experiments, the initial velocities of the samples are equal to 200 m/s. The behavior of clay was described by the MAT_SOIL_AND_FOAM model with the parameters defined earlier. The behavior of the material of the measuring bar was described by a linear elastic model (density 7850 kg/m^3, the Young modulus 185 GPa and Poisson's ratio 0.28).

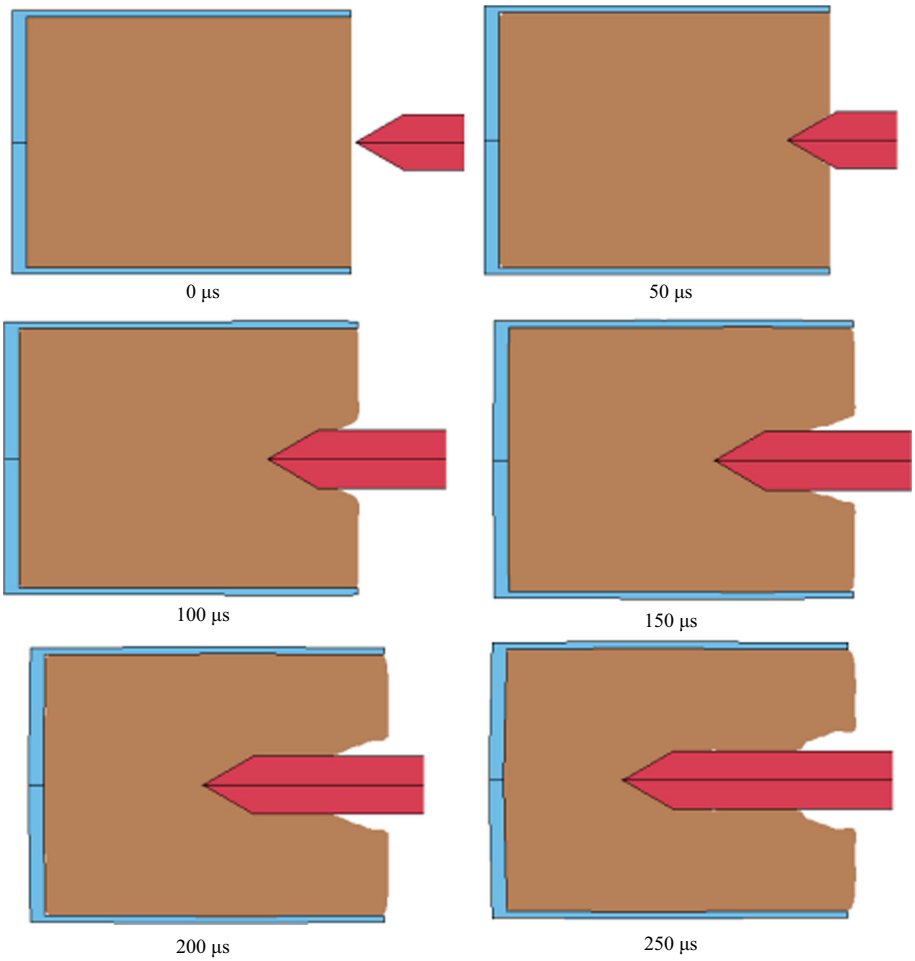

Fig. 8 Process of impact interaction of the bar with clay

The problem was solved in an axisymmetric formulation. An explicit scheme was used to integrate the equations in time. The simulation of the container and the measuring bar was carried out by Lagrangian reference frame using area-weighted axisymmetric finite elements (type 14). Since large deformations occur in the clay sample during the impact interaction with the measuring bar, the integration of the equations for the sample was carried out in Euler reference frame using the MMALE (multi-material arbitrary Lagrange–Euler) formulation. The interaction of Lagrangian and Eulerian parts was carried out using a special contact CONSTRAINED_LAGRANGE_IN_SOLID. As in the full-scale test, the measuring bar had zero initial velocity, and the parts of the model representing the sample and container were given initial velocities equal to the throwing speed in the full-scale test. The Eulerian grid had the ability to shift in space in the direction of the axis of the bar following the center of mass of the sample material (control card ALE_REFERENCE_SYSTEM_GROUP). This technique allows you to significantly save on computational resources, because there is no need to cover a large area of space with an Eulerian grid and you can cover only the area in close proximity to the sample and increase the accuracy of calculations, since fewer computational errors occur when integrating the mass conservation equation when material flows from cell to cell.

Figure 8 shows the configurations of the computational domain at various time points in a simulation.

Obviously, the force of the penetration resistance of the bar into the clay depends on the coefficient of friction. Besides, as it was shown earlier, the values of the ultimate strength (yield strength) of the material at zero limiting pressure have a certain spread. Since the value of the coefficient of friction for dynamic contact is not exactly known, calculations were carried out with different values of the coefficient of friction (α =0, 0.25, 0.5, 0.75 and 1). To assess the effect of the variation of the initial yield strength of clay on the simulation result, this value also varied from 15 to 25 MPa in simulation. A comparison of the time dependences of the

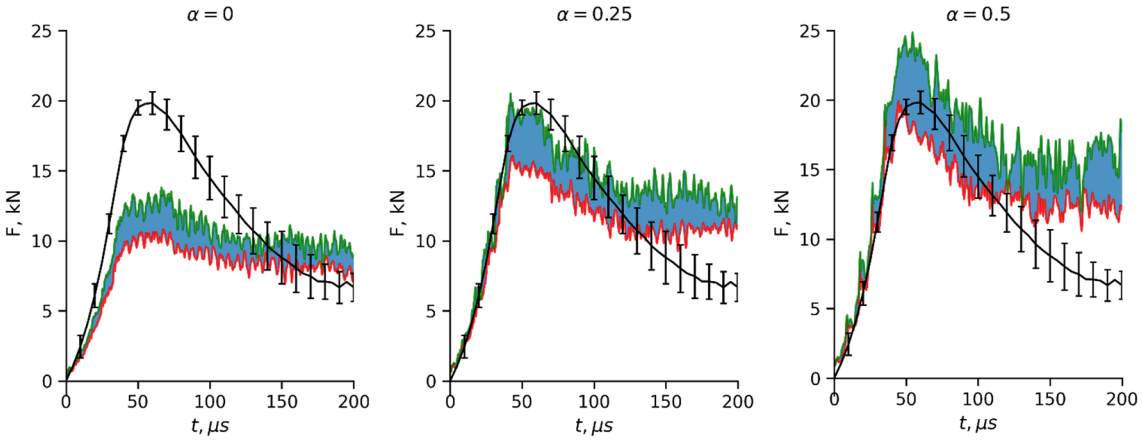

Fig. 9 Calculations for different coefficients of friction (0, 0.25, 0.5)

resistance forces obtained in a full-scale experiment (black line) and computational experiments (colored lines taking into account the spread of values of uniaxial tensile strength) is shown in Fig. 9. The red lines show the dependences of the resistance forces obtained at a yield strength value of 15 MPa and the green lines at a value of 25 MPa.

Numerical simulation has shown that an increase in the coefficient of friction greater than 0.5 does not lead to a change in the calculated time dependence of the penetration resistance force. With a coefficient of friction close to 0.5, the values of the resistance forces measured in the experiment and obtained in the simulation turned out to be quite close: The loading branch, maximum force values and unloading branch practically coincide up to a time of about 100 microseconds, taking into account the spread of material characteristics and experimental data.

It should be noted that the model used does not allow taking into account the influence of the strain rate on the strength characteristics of clay. Therefore, in the calculations, a certain average value was used for the entire area occupied by the material. In reality, different zones of the sample are deformed at different strain rates, and the maximum strain rate takes place in the contact zone of the measuring bar and the sample. For more realistic modeling, it is necessary to use a model that takes into account the effect of the strain rate on the properties of the material, as well as experimentally determine the strain rate dependence of the strength of the material under uniaxial compression in a wider range of loading conditions.

5 Conclusions

Using various variants of the Kolsky (SHPB) method, a study of the dynamic deformation of dry clay soil was carried out. Based on the results of this study, the parameters of the Grigoryan model were determined. To verify this model, reversed ballistic experiments were carried out on the impact interaction of a dry clay barrier with a conical head at an impact velocity of 200 m/s. Numerical calculations were carried out using the LS-Dyna code. The Coulomb friction coefficient 0.5 gives the best match of the numerical and experimental data. A comparison of the results of numerical simulations and real experiments showed that they are quite close within 100 microseconds from the beginning of the collision. Beyond this point, the results of the numerical calculation are higher than the results of the reversed experiments. In our opinion, this phenomenon can be explained by the dependence of the initial strength of clay on the strain rate. The initial compressive strength of clay at strain rates less than $1000\,s^{-1}$ can be significantly less than 20 MPa, which will lead to a decrease in the resistance force with a decrease in the penetration rate and, accordingly, the strain rate of the soil medium. In addition, it is possible that the dry friction coefficient is not constant, and also depends on the penetration rate.

Based on the above, it can be concluded that Grigoryan's model of the soil environment with experimentally determined parameters adequately describes the initial stage of the impact interaction of a conical head with a barrier of dry clay. To refine the model, it is necessary to conduct additional studies of the effect of the strain rate on the initial compressive strength and to take this dependence into account in the model of the soil medium.

Acknowledgements The work was financially supported by the Strategic Academic Leadership Program Priority 2030 (internal number H-496-99_2021-2023).

References

1. Forrestal, M.J., Luk, V.K.: Dynamic spherical cavity-expansion in a compressible elastic-plastic solid. Trans. ASME. J. Appl. Mech. **55**(2), 275–279 (1988)
2. Shi, C., Wang, M., Li, J., Li, M.: A model of depth calculation for projectile penetration into dry sand and comparison with experiments. Int. J. Impact Eng. **73**, 112–122 (2014)
3. Ben-Dor, G., Dubinsky, A., Elperin, T.: Engineering models of high speed penetration into geological shields. Central Euro. J. Eng. **1**(4), 1–19 (2014)
4. Kotov, V.L., Bragov, A.M., Balandin, V.V., et al.: Cavity-expansion approximation for projectile impact and penetration into sand. Continuum Mech. Thermodyn. **34**, 395–421 (2022). https://doi.org/10.1007/s00161-021-01062-8
5. Lagunov, V.A., Stepanov, V.A.: Measurements of the dynamic compressibility of sand under high pressures. Zh. Prikl. Mekh. Tekhn. Fiz. (J. Appl. Mech. Tech. Phys.) **1**, 88–96 (1963)
6. Bragov, A.M., Balandin, V.V., Lomunov, A.K., Filippov, A.R.: Determining the impact compressibility of soft soils from reversed test results. Tech. Phys. Lett. **32**(6), 487–8 (2006). https://doi.org/10.1134/S1063785006060101
7. Bragov, A.M., Grushevskii, G.M.: Influence of the moisture content and granulometric composition on the shock compressibility of sand. Tech. Phys. Lett. **19**, 385–6 (1993)
8. Arlery, M., Gardou, M., Fleureau, J.M., Mariotti, C.: Dynamic behaviour of dry and watersaturated sand under planar shock conditions. Int. J. Imp. Eng. **37**, 1–10 (2010). https://doi.org/10.1016/j.ijimpeng.2009.07.009
9. Bragov, A.M., Lomunov, A.K., Sergeichev, I.V., Tsembelis, K., Proud, W.G.: Determination of physicomechanical properties of soft soils from medium to high strain rates. Int. J. Impact Eng. **35**(9), 967–76 (2008)
10. Song, B., Chen, W., Luk, V.: Impact compressive response of dry sand. Mech. Mater. **41**, 777–85 (2009). https://doi.org/10.1016/j.mechmat.2009.01.003
11. Martin, B.E., Chen, W., Song, B., Akers, S.A.: Moisture effects on the high strain-rate behavior of sand. Mech. Mater. **41**, 786–98 (2009). https://doi.org/10.1016/j.mechmat.2009.01.014
12. Martin, B.E., Kabir, M.E., Chen, W.: Undrained high-pressure and high strain-rate response of dry sand under triaxial loading. Int. J. Imp. Eng. **54**, 51–63 (2013). https://doi.org/10.1016/j.ijimpeng.2012.10.008
13. Chapman, D.J., Tsembelis, K., Proud, W.G.: The behavior of water saturated sand under shock-loading. In: Proceedings of the 2006 SEM Annual Conference and Exposition on Experimental and Applied Mechanics. **2**834–40 (2006)
14. Luo, H., Cooper, W.L., Lu, H.: Effects of particle size and moisture on the compressive behavior of dense Eglin sand under confinement at high strain rates. Int. J. Imp. Eng. **65**, 40–55 (2014). https://doi.org/10.1016/j.ijimpeng.2013.11.001
15. Dianov, M.D., Zlatin, N.A., Mochalov, S.M., et al.: Shock compressibility of dry and watersaturated sand. Sov. Tech. Phys. Lett. **2**, 207–8 (1977)
16. Bragov, A.M., Grushevsky, G.M., Lomunov, A.K.: Use of the Kolsky method for studying shear resistance of soils. DYMAT J. **1**(3), 253–259 (1994)
17. Bragov, A.M., Grushevsky, G.M., Lomunov, A.K.: Use of the Kolsky method for confined tests of soft soils. Exper. Mech. **36**, 237–242 (1996)
18. Bragov, A.M., Kotov, V.L., Lomunov, A.K., Sergeichev, I.V.: Measurement of the dynamic characteristics of soft soils using the Kolsky method. J. Appl. Mech. Tech. Phys. **45**(4), 580–5 (2004). https://doi.org/10.1023/B:JAMT.0000030338.66701.e9
19. Omidvar, Mehdi, Iskander, Magued, Bless, Stephan: Stress-strain behavior of sand at high strain rates. Int. J. Impact Eng. **49**, 192–213 (2012). https://doi.org/10.1016/j.ijimpeng.2012.03.004
20. Yang, R., Chen, J., Yang, L., Fang, Sh., Liu, J.: An experimental study of high strain-rate properties of clay under high consolidation stress. Soil Dyn. Earthquake Eng. **92**, 46–51 (2017)
21. He, Y.X., Luan, G.B., Zhu, W.: Dynamic Constitutive modeling of partially saturated clay under impact loading. Int. J. Nonlinear Sci. Numer. Simul. **11**, 195–199 (2010)
22. Gang, Z., Yunliang, L., Jin, L., Zutang, W., Ke, W., Jiyong, J., Shunshun, T., Bingwen, Q., Yurong, Z., Xiangrong, Z.: Dynamic behavior of clay with different water content under planar shock conditions. Int. J. Imp. Eng. **129**, 57–65 (2019). https://doi.org/10.1016/j.ijimpeng.2019.03.001
23. Li, Yunliang, Zhu, Yurong, Zhang, Xiangrong, Li, Jin, Ke, Wu., Jing, Jiyong, Tan, Shushun, Zhou, Gang: Dynamic behavior of remolded loess under planar shock conditions. Int. J. Impact Eng. **111**, 236–243 (2018). https://doi.org/10.1016/j.ijimpeng.2017.09.016
24. Bragov, A.M., Gandurin, V.P., Grushevskii, G.M., Lomunov, A.K.: New potentials of Kol'skii's method for studying the dynamic properties of soft soils. J. Appl. Mech. Tech. Phys **36**(3), 476–481 (1996). https://doi.org/10.1007/BF02369791
25. Bragov, A.M., Demenko, P.V., Kruszka, L., Lomunov, A.K., Sergeichev I.V.: Évaluation de la compressibilité dynamique et de la résistance aucisaillement pour une large gamme de pressions et de vitesses de déformation Investigation of dynamic compressibility and shear resistance of soft soils in a wide range of strain rate and pressure. In: Fifth European Conference "Numerical Methods in Geotechnical Engineering" NUMGE, Mestat (ed.), Presses de l'ENPC/LCPC, Paris, pp. 909-917 (2002)
26. Konstantinov, A., Bragov, A., Igumnov, L., Eremeyev, V., Balandin, V.V., Balandin, V.L.: Experimental study and identification of a dynamic deformation model of dry clay at strain rates up to 2500 s-1. J. Appl. Comput. Mech. **8**(3), 981–995 (2022). https://doi.org/10.22055/JACM.2022.39321.3387
27. Balandin, V.V., Balandin, V.L., Bragov, A.M., Kotov, V.L.: Experimental study of the dynamics of penetration of a solid body into a soil medium. Tech. Phys. **61**(6), 860–868 (2016)

28. Bragov, A.M., Balandin, V.V., Igumnov, L.Á., Èîtov, V.L., Kruszka, L., Lomunov, Á.K.: Impact and penetration of cylindrical bodies into dry and water-saturated sand // Int. J. Imp. Eng. **122**, 197–208 (2018)
29. Omidvar, M., Iskander, M., Bless, S.: Response of granular media to rapid penetration //Int. J. Imp. Eng. **66**, 60–82 (2014)
30. Veldanov, V.A., Markov, V.A., Pusev, V.I., Ruchko, A.M., Sotskii, MYu., Fedorov, S.V.: Computation of non-deformable striker penetration into low strength obstacles using piezoelectric accelerometry data. Tech. Phys. **56**(7), 992–1002 (2011). https://doi.org/10.1134/S1063784211070231
31. Bivin, Yu.K., Viktorov, V.V., Stepanov, L.P.: Study of body motion in a clay environment. MTT **2**, 159–165 (1978)
32. Bivin, Y.K., Viktorov, V.V., Kovalenko, B.Y.: Determination of dynamic characteristics of soils by the penetration method. Mech. Solids **15**(3), 105–110 (1980)
33. Bivin, Yu.K., Kolesnikov, V.A., Flitman, L.M.: Determining mechanical properties of a medium by the dynamic penetration method. Izv. Akad. Nauk SSSR. Mekh. Tverd. Tela **5**, 182–185 (1982). (**[Mech. Solids (Engl. Transl.)**)
34. Buharev, Yu.N., Gandurin, V.P.: Forces acting on a sharp cone in the non-stationary stage of penetration into water and soil. Appl. Prob. Strength Plasticity (in Rus.) **53**, 46–55 (1995)
35. Buharev Yu.N., Gandurin V.P., Korablev A.E., Morozov V.A., Himovich M.I.: An experimental study of the penetration of an undeformable striker into clay and snow. Appl. Prob. Strength Plasticity (in Rus.). 99–106 (1991)
36. Buharev, Yu.N., Korablev, A.E., Himovich, M.I.: Experimental determination of shear stresses on the surface of the impactor during dynamic penetration into the soil. Mech. Solids (In Rus.) **2**, 186–188 (1995)
37. Balandin, V.V., Balandin, Vl.Vl., Bragov, A.M.: Experimental study of the processes of penetration of axisymmetric bodies into soft soil media/Nizhny Novgorod, ISBN 978-5-600-02899-9, P.163 (in Rus) (2020)
38. Dayal, U., Allen, J.H., Reddy, D.V.: Low velocity projectile penetration of clay. J. Geotherm Eng. Div. **8**, 919–937 (1980)
39. Kolsky, H.: An investigation of the mechanical properties of materials at very high rates of loading. Proc. Phys. Soc. Lond. B **62**, 676–700 (1949)
40. Grigoryan, S.S.: Basic concepts of soil dynamics. J. Appl. Math. Mech. **24**(6), 1057–1072 (1960). ((**In Rus)**)
41. Bazhenov, V.G., Balandin, V.V., Grigoryan, S.S., Kotov, V.L.: Analysis of models for calculating the motion of solids of revolution of minimum resistance in soil media. J. Appl. Math. Mech. **78**(1), 65–76 (2014). https://doi.org/10.1016/j.jappmathmech.2014.05.008
42. LS-DYNA Keyword User's Manual, Vol. II, Material Models, LS-DYNA R11 10/12/18 (r:10572), Livermore Software Technology Corporation (LSTC, p.178-182)
43. Dyanov, D.Y., Kotov, V.L.: Determination of nonlinear strength characteristics of sandy soil based on the Grigoryan soil model. Prob. Strength Plast. **82**, 471–482 (2020). https://doi.org/10.32326/1814-9146-2020-82-4-471-482